

## Segregation, core alloying, and shape transitions in bimetallic nanoclusters: Monte Carlo simulations

F. Calvo, E. Cottancin, and M. Broyer

*LASIM, Université Claude Bernard Lyon 1, 43 Boulevard du 11 Novembre 1918, F69622 Villeurbanne Cedex, France*

(Received 6 February 2008; revised manuscript received 5 March 2008; published 28 March 2008)

The stable structures and melting behaviors of silver-rich bimetallic clusters  $(\text{Ag}_{0.75}M_{0.25})_N$ , where  $M=\text{Au}$ , Pt, and Ni, and containing up to  $N=309$  atoms, were investigated by exchange Monte Carlo simulations. Ag-Au clusters are stable as a solid solution equilibrium phase below their melting point. Ag-Pt clusters exhibit a continuous transition from core/shell to alloy core/pure Ag shell. Ag-Ni clusters display a peculiar transformation to prolate shapes before the nickel core melts by alloying with silver at higher temperatures. All of these results are consistent with available experimental measurements.

DOI: [10.1103/PhysRevB.77.121406](https://doi.org/10.1103/PhysRevB.77.121406)

PACS number(s): 64.70.Nd, 36.40.Ei, 61.46.Bc

Metal nanoparticles play an increasingly important role not only in materials science, but also in chemistry, biology, and even medicine. Tailoring the properties of nanoparticles is possible not only by reducing the size, thereby increasing the surface to volume ratio, but also by mixing several metals together. Nanometer scale bimetallic particles have been used for their enhanced catalytic,<sup>1</sup> magnetic,<sup>2</sup> or electronic and optical<sup>3</sup> properties. Particles made up of noble metals, in particular, display a surface plasmon resonance (SPR) near the visible range, which has been exploited in biomedical applications for drug delivery, antibacterial activity, or cancer diagnosis and treatment.<sup>4</sup>

The synthesis of metallic nanoclusters relies on two main approaches. Physical methods proceed by laser irradiation of bulk precursors (rods, surfaces, or powders) and subsequent thermodynamically driven aggregation in the gas or liquid phases. In chemical methods, the nanoparticles are formed by the reduction of metal salts into metal atoms, using thiols as stabilizers, with the growth kinetics being then strongly influential.<sup>5</sup> For bimetallic particles, one current challenge lies in the production and characterization of particles with well-defined sizes and shapes, with fully mixed nanoalloys and fully segregated nanocomposites as two extreme cases.

In this Rapid Communication, we show by means of numerical simulations how temperature affects the alloying properties of some bimetallic clusters at equilibrium, for different silver-rich particles containing miscible (Au, Pt) or immiscible (Ni) elements.<sup>6</sup> The three additional metals chosen here lead to strongly contrasted behaviors ranging from core/shell to alloy core/pure shell and, finally, to homogeneous alloys. We also find evidence that Ag-Ni clusters undergo a preliminary shape transition toward highly deformed prolate structures before eventually melting.

From the theoretical perspective, first-principle approaches are currently feasible only in the small size limit,<sup>7</sup> and they are usually appropriate for addressing the stable structures and segregation issues. Conversely, very large clusters containing several thousand atoms can be addressed at the statistical level by simplifying the interactions down to discrete Ising-like models.<sup>8</sup> Melting in medium size bimetallic clusters has been studied by using approximate quantum descriptions,<sup>9,10</sup> but most often by semiempirical potentials<sup>11,12</sup> generally employing molecular dynamics.

The nanoparticles investigated here are made from silver and another metal  $M=\text{Au}$ , Pt, or Ni. We focus on the 3:1 silver concentration, initially chosen for a comparison with available experiments.<sup>13–15</sup> The cluster sizes range from 55 to 309 atoms, covering 2–4 icosahedral shells. In order to sample the phase space efficiently, including the many possible alloyed forms, explicit many-body potentials are used to model the interactions among metal atoms within the framework of Monte Carlo (MC) simulations in the canonical ensemble. These potentials are all based on the second moment approximation in tight-binding theory, and the functional forms and parameters can be found in Ref. 16 for Ag-Au, in Ref. 17 for Ag-Pt, and in Ref. 18 for Ag-Ni clusters, respectively.

In addition to conventional displacement moves, random identity swap moves are attempted with a fixed probability of 10%. These moves consist of swapping two unlike atoms Ag and  $M$ , in the bimetallic cluster. Such moves have been shown to be rather unfavorable at low temperatures in binary glass forming materials<sup>19</sup> due to the difficulty of inserting the larger atom in the cavity of the smaller atom. A possible way to circumvent this problem is through configurational bias.<sup>19</sup> Here, we extended the preferential sampling scheme of Owicki and Scheraga<sup>20</sup> by selecting the Ag- $M$  pairs having higher chances of being swapped, correcting for this bias afterward in the acceptance rate. The selection is based on a distance criterion, with the  $(i, j)$  pair being given a weight  $p_{ij}=r_{ij}^\nu$ , where  $r_{ij}$  is the distance between atoms  $i$  and  $j$ , and  $\nu=2$  is a fixed exponent. After one  $M$  atom is randomly selected, denoted as  $i$ , all distances  $r_{ij}$  to Ag atoms ( $j$ ) are computed and atom  $j$  is randomly drawn from the normalized weights  $p_{ij}/W_{\text{old}}^{(i)}$ , with  $W_{\text{old}}^{(i)}=\sum_k p_{ik}$ . The atoms  $i$  and  $j$  are then swapped and new weights  $p'_{ik}$  and their sum  $W_{\text{new}}^{(i)}=\sum_k p'_{ik}$  are calculated. The swapping move is finally accepted according to a Metropolis rule, in which the Boltzmann term is multiplied by the correcting factor  $W_{\text{old}}^{(i)}/W_{\text{new}}^{(i)}$ .<sup>20</sup> The various Monte Carlo trajectories at different temperatures are then carried out simultaneously, with two adjacent trajectories possibly exchanging their configurations in the parallel tempering strategy.<sup>21</sup> The most stable structures found at low temperatures are all icosahedral. However, as will be discussed below, substituting silver atoms into nickel leads to significant deformations.

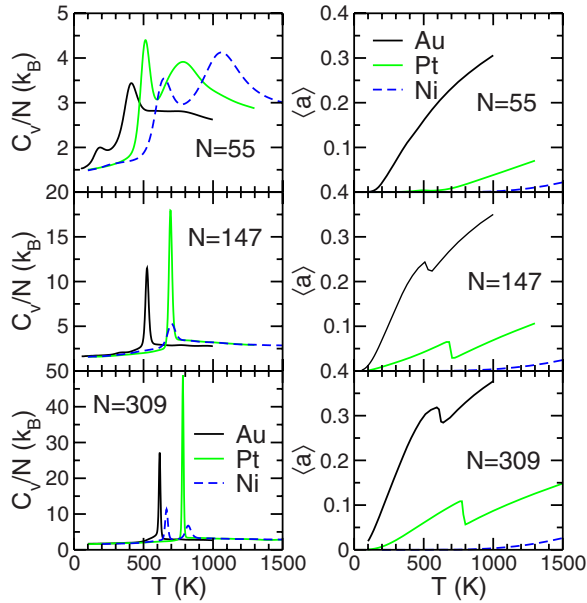


FIG. 1. (Color online) Canonical heat capacity (left panel) and average acceptance of identity swapping moves (right panel) of  $(\text{Ag}_{0.75}\text{M}_{0.25})_N$  clusters, with  $N=55$ , 147, and 309. The black, green (light gray), and dashed blue (dark gray) curves are for  $M=\text{Au}$ , Pt, and Ni, respectively.

The equilibrium heat capacities of all clusters are presented in Fig. 1 as a function of temperature. As a general measure of the alloying extent in the particles, we have reported the average acceptance rates  $\langle a \rangle$  of identity swapping moves obtained from the MC trajectories. Though not a physical observable, we have found this quantity to be more sensitive to temperature than the usual short- and long-range order parameters defined for specific lattice symmetries.<sup>22</sup>

The heat capacities show broad peaks for small clusters, which shift to higher temperatures and become narrower in larger systems, as expected. In agreement with the bulk phase diagram<sup>6</sup> and with simulation results by Mottet *et al.*<sup>11</sup> the melting temperatures of the alloyed (Ag-Au and Ag-Pt) and immiscible (Ag-Ni) clusters are found to be higher than those of the pure Ag clusters.<sup>23</sup> The premelting peaks found in the 55-atom clusters, which can even exceed the melting peak for Ag-Pt, have no counterpart in pure silver clusters. They convey the different onsets of alloying (Ag-Au and Ag-Pt) or partial melting (silver shell in Ag-Ni) about which we shall focus on hereafter. As the cluster size increases, the peaks soften and become low-temperature shoulders. In the case of Ag-Ni, the finite-size effects are stronger and non-monotonic. In particular, the 309-atom cluster exhibits two clear peaks at 670 and 810 K. The influence of temperature on alloying, as indicated by the statistical average  $\langle a \rangle$ , is very different for gold, platinum, and nickel, but size does not play a strong role. It is quite easy to mix Ag and Au atoms, even at room temperature. Mixing Ag with Pt can also be achieved; however, in the case of Ag-Ni, only very high temperatures lead to (occasional) mixing. These latter results are, of course, consistent with the known bulk phase diagram of these binary metals.<sup>6</sup> In the larger Ag-Au and Ag-Pt clusters, the numerous surface rearrangements appear to slightly

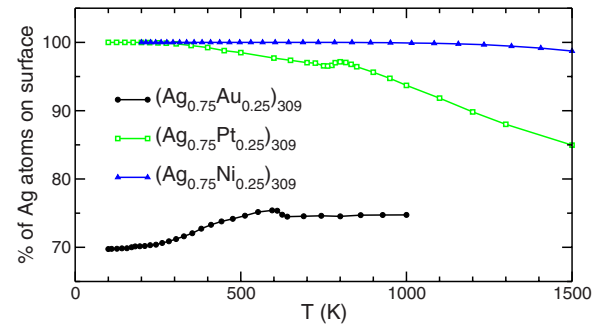


FIG. 2. (Color online) Number of silver atoms on the surface of  $(\text{Ag}_{0.75}\text{M}_{0.25})_{309}$  clusters,  $M=\text{Au}$ , Pt, and Ni, relative to the total number of surface atoms.

restrain the chances of successfully swapping atoms, as seen on the small but sharp drop in the average acceptance near the melting point.

Figure 1 cannot provide a complete picture of the equilibrium properties of the nanoparticles without further structural analysis. The surface compositions of the nanoparticles have been obtained from the simulations, assuming that surface atoms have a coordination number lower than 10. The variations of the ratio of silver surface atoms are presented in Fig. 2 for the 309-atom clusters.

As in the bulk alloys,<sup>6</sup> Ag-Au clusters have a strong tendency to mix, even at low temperature. This is due to the very similar Wigner-Seitz radii (and not too dissimilar surface energies) of these metals.<sup>24</sup> Conversely, both Ag-Ni and Ag-Pt clusters have a pure silver outer shell at room temperature. Above 350 K, Pt atoms begin to partially alloy with the surface and, above the melting point, the ratio smoothly decreases toward the expected bulk concentration of 3/4. These results are consistent with the higher surface energies of nickel and platinum,<sup>24</sup> and agree with experimental measurements on Ag-Au (Ref. 13) and Ag-Ni (Ref. 14) clusters.

To get further insight into the differences between Ag-Au and Ag-Pt clusters, the equilibrium radial distribution functions have been calculated at 305 K, again for the larger 309-atom clusters. These quantities are reported in Fig. 3 as a function of the distance from the cluster center of mass.

In Ag-Au clusters, the distributions of both metals extend over the entire volume and overlap with each other, further indicating that the stable phase is a homogeneous alloy. Considering that the acceptance rate of swap moves is already high at this temperature ( $>20\%$  from Fig. 1), the equilibrium state should be better described as a solid solution consisting of a large number of energetically close isomers, rather than a single well-defined mixed structure. The random alloy found as the lowest *free* energy state was shown to correctly account for the optical properties of silver-gold nanoparticles.<sup>13</sup>

In Ag-Pt clusters, the most stable 0 K geometries found with the present empirical model are icosahedral, with a Pt core surrounded by a Ag shell. At the rather low temperature of 305 K, the radial distribution functions overlap up to about 8 Å from the cluster center of mass, with the outer layer being made of pure silver. A snapshot of a typical configuration taken at this temperature, shown as an inset of Fig.

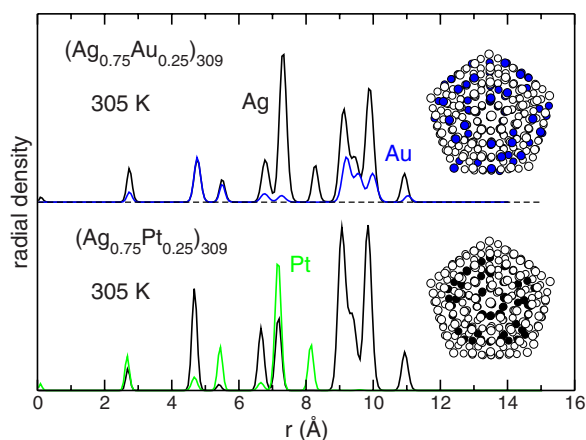


FIG. 3. (Color online) Radial atomic densities of silver, gold, and platinum atoms in the four-shell clusters  $(\text{Ag}_{0.75}\text{Au}_{0.25})_{309}$  (upper panel) and  $(\text{Ag}_{0.75}\text{Pt}_{0.25})_{309}$  (lower panel) obtained at 305 K. Typical configurations of the clusters, with silver atoms as white balls, are shown in the right part of the figure.

3, illustrates that only silver atoms cover the surface. The first icosahedral layer (including the central atom) is fully alloyed and the second and third layers are partially alloyed. This geometrical overlap and the non-negligible acceptance rate of swap moves characterize the equilibrium phase as an alloy core/pure shell structure. As in Ag-Au clusters, the alloyed part should be more appropriately described as a solid solution. By comparing the two radial distributions in Fig. 3, the peaks are narrower and better resolved for the platinum alloy with respect to the Ag-Au cluster. This higher degree of ordering is consistent with the higher melting point of the former system.

To our knowledge, alloy core/pure shell *equilibrium* structures such as those found here for silver-platinum nanoparticles have never been reported in the literature, although Zhou *et al.*<sup>25</sup> were able to synthesize similar Cu-Pt clusters. Interestingly, pure core/alloy shell Cu-ZnO particles have been reported by Hambrock *et al.*<sup>26</sup> as well. In the present Ag-Pt case, a direct evidence by electronic microscopy, though it may be possible, remains difficult and is still lacking. However, the optical absorption spectra of Ag-Pt recorded at increasing platinum concentration do not exhibit the SPR predicted by the Mie theory assuming a dielectric function built from those of the pure constituents.<sup>15</sup> Complementary low-energy ion scattering measurements show that the surface of these cluster is enriched in silver.<sup>15</sup> Our results indicate alloy core/pure shell configurations as another possibility that could explain these observations. This assumption could be verified by using x-ray absorption fine structure experiments.<sup>27</sup>

As seen from both the average acceptance  $\langle a \rangle$  or the ratio of surface silver atoms and by monitoring the radial distributions, the transition to partially alloyed structures is very gradual in Ag-Pt clusters, but does not have a clear thermodynamical signature on the heat capacity, except for a mere but soft increase. This continuous transition could then be an example of the long sought second-order phase transition rounded by size effects.<sup>28</sup>

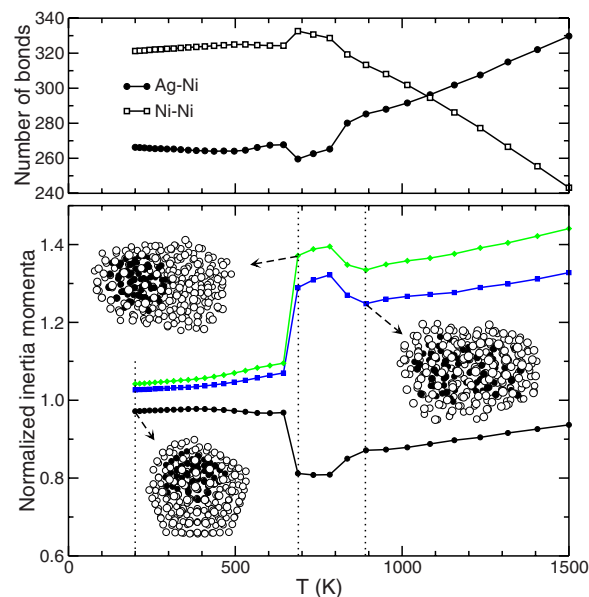


FIG. 4. (Color online) Average number of Ag-Ni and Ni-Ni bonds (upper panel) and average inertia momenta normalized by their  $T=0$  value (lower panel) for the cluster  $(\text{Ag}_{0.75}\text{Ni}_{0.25})_{309}$ . Some snapshots illustrate the stable structure, shape transformation, and core melting of the cluster, with silver atoms being represented as white balls.

The analysis of the radial distributions for Ag-Ni clusters turned out to be less insightful. The most stable structures are, indeed, of the core/shell type for all sizes, which is in agreement with other theoretical investigations.<sup>29</sup> However, the pronounced size mismatch between the two metals leads to a shift in the nickel core with respect to the cluster center of mass, resulting in a deformation of the icosahedral silver shell seen in the lower inset of Fig. 4. A visual inspection suggests monitoring specific geometrical properties related to the connectivity and global shape for these clusters. Figure 4 shows the variations of the thermally averaged number of Ag-Ni and Ni-Ni bonds in the 309-atom cluster as a function of temperature, as well as the average inertia momenta normalized to their value in the global minimum. As temperature varies in the 200–660 K range, the cluster undergoes some thermal motion and keeps its spherical shape. At about 680 K, strong changes in the inertia momenta indicate a transition to prolate geometries. The high heat capacity peak at this temperature marks the onset of a finite-size first-order phase change, related here to the melting of the silver shell. By comparing the higher melting point obtained for the silver shell with respect to the pure 309-atom Ag cluster,<sup>23</sup> the nickel core is found to have a significant stabilizing role.

The present temperature-induced shape transition allows the nickel core to make more bonds, at the expense of the outer, melted silver part. In other words, the strain experienced by the Ni core is released at the expense of a lesser strain gained by the outer shell. As 810 K is reached, the inertia momenta become closer to each other and the numbers of Ag-Ni and Ni-Ni bonds increase and decrease, respectively. Snapshots represented as insets in Fig. 4 show that the nickel core remains stable in the intermediate range

of 680–810 K, but melts by alloying with silver above 810 K. An inherent structures analysis confirms the disordered and alloyed character of the cluster configurations at these temperatures. The shape transition found here for Ag-Ni nanoparticles is a peculiar manifestation of cluster thermodynamics, which has not been reported before. It could explain why bimetallic clusters of similar immiscible elements such as Ag-Cu are experimentally found as core/shell, but with strongly deformed prolate shapes.<sup>30</sup>

In summary, the bimetallic clusters investigated in this Rapid Communication cover the ranges of segregated nanocomposites to mixed nanoalloys. An alloy core/pure shell

phase was found here for Ag-Pt particles at equilibrium in a broad temperature range. Our investigation also showed that clusters of elements having a strong size mismatch can exhibit a shape transformation toward prolate geometries triggered by the core releasing its strain. These theoretical findings are supported by several experimental measurements. The present simulation methods could provide candidate structures to be checked at higher levels of theory. They would also be valuable for studying other compositions and different alloys, paving the way for finite-size phase diagrams.<sup>31</sup>

- <sup>1</sup>S. Arrii, F. Morfin, A. J. Renouprez, and J.-L. Rousset, *J. Am. Chem. Soc.* **126**, 1199 (2004).
- <sup>2</sup>S. H. Sun, C. B. Murray, D. Weller, L. Folks, and A. Moser, *Science* **287**, 1989 (2000).
- <sup>3</sup>A. N. Shipway, E. Katz, and I. Willner, *ChemPhysChem* **1**, 18 (2000).
- <sup>4</sup>C. Loo, A. Lowery, N. Halas, J. West, and R. Drezek, *Nano Lett.* **5**, 709 (2005); A. Panáček, L. Kvítek, R. Prucek, M. Kolář, R. Večeřová, N. Pizúrová, V. K. Sharma, T. Nevěčná, and R. Zbořil, *J. Phys. Chem. B* **110**, 16248 (2006); X. H. Huang, P. K. Jain, I. H. El-Sayed, and M. A. El-Sayed, *Nanomedicine* **2**, 681 (2007).
- <sup>5</sup>F. Baletto and R. Ferrando, *Rev. Mod. Phys.* **77**, 371 (2005).
- <sup>6</sup>T. B. Massalski, J. L. Murray, L. H. Bennett, and H. Baker, *Binary Alloy Phase Diagrams* (American Society for Metals, Metals Park, OH, 1986), Vol. 1.
- <sup>7</sup>See, e.g., H. Y. Kim, H. G. Kim, J. H. Ryu, and H. M. Lee, *Phys. Rev. B* **75**, 212105 (2007).
- <sup>8</sup>F. Lequien, J. Creuze, F. Berthier, and B. Legrand, *J. Chem. Phys.* **125**, 094707 (2006).
- <sup>9</sup>A. Aguado, L. E. González, and J. M. López, *J. Phys. Chem. B* **108**, 11722 (2004).
- <sup>10</sup>M. S. Lee, S. Gowtham, H. Y. He, K. C. Lau, L. Pan, and D. G. Kanhere, *Phys. Rev. B* **74**, 245412 (2006).
- <sup>11</sup>C. Mottet, G. Rossi, F. Baletto, and R. Ferrando, *Phys. Rev. Lett.* **95**, 035501 (2005).
- <sup>12</sup>F. Y. Chen, B. C. Curley, G. Rossi, and R. L. Johnston, *J. Phys. Chem. C* **111**, 9157 (2007).
- <sup>13</sup>M. Gaudry, J. Lermé, E. Cottancin, M. Pellarin, J.-L. Vialle, M. Broyer, B. Prével, M. Treilleux, and P. Mélinon, *Phys. Rev. B* **64**, 085407 (2001).
- <sup>14</sup>M. Gaudry, E. Cottancin, M. Pellarin, J. Lermé, L. Arnaud, J. R. Huntzinger, J. L. Vialle, M. Broyer, J. L. Rousset, M. Treilleux, and P. Mélinon, *Phys. Rev. B* **67**, 155409 (2003).
- <sup>15</sup>E. Cottancin, M. Gaudry, M. Pellarin, J. Lermé, L. Arnaud, J. R. Huntzinger, J.-L. Vialle, M. Treilleux, P. Mélinon, J.-L. Rousset, and M. Broyer, *Eur. Phys. J. D* **24**, 111 (2003).
- <sup>16</sup>G. Rossi, R. Ferrando, A. Rapallo, A. Fortunelli, B. C. Curley, L. D. Lloyd, and R. L. Johnston, *J. Chem. Phys.* **122**, 194309 (2005).
- <sup>17</sup>H. Rafii-Tabar and A. P. Sutton, *Philos. Mag. Lett.* **63**, 217 (1991).
- <sup>18</sup>F. Baletto, C. Mottet, and R. Ferrando, *Phys. Rev. Lett.* **90**, 135504 (2003).
- <sup>19</sup>R. Faller and J. J. de Pablo, *J. Chem. Phys.* **119**, 4405 (2003); E. Flenner and G. Szamel, *Phys. Rev. E* **73**, 061505 (2006).
- <sup>20</sup>J. C. Owicki and H. A. Scheraga, *Chem. Phys. Lett.* **47**, 600 (1977).
- <sup>21</sup>The simulations were carried out by using 32 replicas in the temperature ranges of 50–1000 K for Ag-Au, and 100–1500 K for Ag-Pt and Ag-Ni clusters, respectively. The temperatures were initially allocated according to a geometric progression, and then refined near the transition temperatures. Each trajectory consisted of several runs of  $10^6$  cycles per replica following  $5 \times 10^5$  thermalization cycles, repeated until convergence. Being a global optimization method, exchange MC also provides low-energy structures as a by-product during the first stages of the simulation. These putative global minima were refined by basin-hopping Monte Carlo+minimization searches with many identity swapping moves.
- <sup>22</sup>J. M. Cowley, *Phys. Rev.* **77**, 669 (1950).
- <sup>23</sup>F. Calvo (unpublished).
- <sup>24</sup>C. L. Yaws, *Chemical Properties Handbook: Physical, Thermodynamic, Environmental, Transport, Safety, and Health Related Properties for Organic and Inorganic Chemicals* (McGraw-Hill, New York, 1999).
- <sup>25</sup>S. Zhou, B. Varughese, B. Eichhorn, G. Jackson, and K. McIlwrath, *Angew. Chem., Int. Ed.* **44**, 4539 (2005).
- <sup>26</sup>J. Hambrock, M. K. Schröter, A. Birkner, C. Wöll, and R. A. Fischer, *Chem. Mater.* **15**, 4217 (2003).
- <sup>27</sup>D. Lahiri, B. Bunker, B. Mishra, Z. Zhang, D. Meisel, C. M. Doudna, M. F. Bertino, F. D. Blum, and A. T. Tokuyoshi, *J. Appl. Phys.* **97**, 094304 (2005).
- <sup>28</sup>A. Proykova and R. S. Berry, *Z. Phys. D: At., Mol. Clusters* **40**, 215 (1997).
- <sup>29</sup>A. Rapallo, G. Rossi, R. Ferrando, A. Fortunelli, B. C. Curley, L. D. Lloyd, G. M. Tarbuck, and R. L. Johnston, *J. Chem. Phys.* **122**, 194308 (2005).
- <sup>30</sup>M. Cazayous, C. Langlois, T. Oikawa, C. Ricolleau, and A. Sacuto, *Microelectron. Eng.* **84**, 419 (2007).
- <sup>31</sup>M. Wautelet, J.-P. Dauchot, and M. Hecq, *Nanotechnology* **11**, 6 (2000).